

XMM-Newton observations of GB B1428+4217: confirmation of intrinsic soft X-ray absorption

M. A. Worsley^{1*}, A. C. Fabian¹, A. Celotti² and K. Iwasawa¹

¹*Institute of Astronomy, Madingley Road, Cambridge CB3 0HA*

²*S. I. S. S. A., via Beirut 2-4, I-34014 Trieste, Italy*

22 November 2018

ABSTRACT

We report the results of *XMM-Newton* observations of the X-ray bright, radio-loud blazar GB B1428+4217 at a redshift of $z = 4.72$. We confirm the presence of soft X-ray spectral flattening at energies $\lesssim 0.7$ keV as reported in previous *ROSAT* and *BeppoSAX* observations. At hard X-ray energies the spectrum is consistent with a power-law although we find the spectral slope varied between both *XMM-Newton* observations and is also significantly different from that reported previously. Whilst we cannot rule-out intrinsic cold absorption to explain the spectral depression, we favour a dust-free warm absorber. Cold absorption requires a column density $\sim 1.4 - 1.6 \times 10^{22} \text{ cm}^{-2}$ whilst a warm absorber could have up to $\sim 10^{23} \text{ cm}^{-2}$ and an ionization parameter $\sim 10^2$. The spectrum of GB B1428+4217 shows remarkable parallels with that of the $z = 4.4$ blazar PMN J0525–3343, in which the available evidence is also most consistent with a warm absorber model.

Key words: galaxies: active – galaxies: individual: GB B1428+4217 – X-rays: galaxies.

1 INTRODUCTION

High-redshift quasars are important objects in the study of the early evolution of massive black holes and the interaction with their host galaxies. A number of radio-loud quasars have been found to show the spectral characteristics typical of blazars. GB B1428+4217 at $z = 4.72$ (Hook & McMahon 1998; Fabian et al. 1997, 1998, 1999) displays spectral flattening at soft X-ray energies in *ROSAT* (Boller et al. 2000) and *BeppoSAX* (Fabian et al. 2001a) data. Here we confirm the flattening with *XMM-Newton* observations. Soft X-ray flattening has also been reported from RX J1028.6–0844 (Yuan et al. 2000) and PMN J0525–3343 (Fabian et al. 2001b) at redshifts of $z = 4.28$ and $z = 4.4$ respectively. *XMM-Newton* data shows only marginal evidence for flattening in the case of RX J1028.6–0844 (Grupe et al. 2004). Conversely, the effect has been confirmed in PMN J0525–3343 (Worsley et al. 2004). Spectral flattening is consistent with a trend seen in a number of studies of lower-redshift radio-loud quasars (e.g. Cappi et al. 1997; Fiore et al. 1998; Reeves & Turner 2000).

The most consistent explanation for the flattening is intrinsic absorption with column densities of the order $10^{22-23} \text{ cm}^{-2}$. Intergalactic absorption systems remain an unlikely possibility given their low metallicities. Furthermore, in order to account for the flattening the line of sight to the blazar would need to intercept two or more very high column density systems of which the probability is very low. Certainly this explanation cannot account for the spectral

depressions seen in an increasing number of objects. An alternative explanation for flattening is a break in the underlying blazar continuum. Hard X-ray production in blazars is likely to be due to the inverse Compton scattering of seed photons by relativistic electrons in the jet. A spectral break can arise through a low energy cut-off in the electron population or by a peaked seed photon spectrum, however the break appears much too sharp for this to be plausible.

Given an intrinsic absorber hypothesis there remains much discussion about the nature of the absorber. X-ray data alone have been unsuccessful in breaking the degeneracy between a cold (neutral) absorber or one that is warm (ionized). Optical observations however, can play a crucial role in this regard. A number of the blazars showing soft X-ray flattening have optical spectra (corresponding to rest frame UV emission) which indicate very little dust along the line of sight or show any evidence of a Lyman-limit system (for the optical data for GB B1428+4217 and PMN J0525–3343 see Hook & McMahon 1998 and Péroux et al. 2001). These point to a dust-free yet metal-enriched absorber where hydrogen has been ionized, consistent with the warm absorber such as that seen in Seyfert galaxies (e.g. Reynolds 1997; Crenshaw et al. 1999). Strong intrinsic C IV absorption is common in these galaxies and it is also a feature of PMN J0525–3343.

2 PREVIOUS OBSERVATIONS

GB B1428+4217 was discovered by Hook & McMahon (1998) in an optical survey for high-redshift quasars. An X-ray follow-up was conducted by Fabian et al. (1997) with the *ROSAT* HRI and *ASCA*

* E-mail: maw@ast.cam.ac.uk

Table 1. Details of *XMM-Newton* observations.

Revolution	Date	Good Exposure Times (s)		
		PN	MOS-1	MOS-2
549	2002 Dec 09	2625	4055	4260
569	2003 Jan 17	11534	14241	14235

(Fabian et al. 1998). Spectral fits were consistent with a power-law continuum with a photon index $\Gamma = 1.29$ although the *ASCA* SIS data alone were suggestive of some excess absorption. Subsequent *ROSAT* observations showed that X-ray flux varied by a factor of two over a time-scale of around 2.5 days in the rest frame of the source. Radio data also shows variability, with amplitudes of $\sim 40/15$ per cent on rest frame time-scales of weeks/days.

More evidence of X-ray variability was seen in a *ROSAT* PSPC observation (Boller et al. 2000), where changes of ~ 25 per cent occur on rest frame timescales of 1.8 hours. The low-energy sensitivity of the PSPC detector clearly revealed a spectral depression in the soft X-ray band, consistent with an absorbing column density of $N_{\text{H}} \sim 1.5 \times 10^{22} \text{ cm}^{-2}$ (if intrinsic to the source).

Spectral flattening was further confirmed by *BeppoSAX* (Fabian et al. 2001a). The fitted spectrum was that of a $\Gamma = 1.45$ power-law with an intrinsic absorption column density of $N_{\text{H}} \sim 8 \times 10^{22} \text{ cm}^{-2}$. Warm absorption models were considered, with column densities of order $N_{\text{H}} \sim 10^{23.3} \text{ cm}^{-2}$ and ionization parameters of order $\xi \sim 10^2$ being marginally consistent with results from *BeppoSAX* as well as those from the previous *ROSAT* and *ASCA* observations.

3 XMM-NEWTON OBSERVATIONS

3.1 Data reduction

XMM-Newton observed GB B1428+4217 on 2002 December 9 and again on 2003 January 17 (Table 1). All observations were performed in full frame imaging mode with the thin filter. The EPIC data reduction was performed with the Scientific Analysis Software (SAS) v5.4.1. Periods of background flaring were excluded and the data were filtered in the standard way to include only the recommended events for spectral analysis (Ehle et al. 2003) i.e. using the event pattern ranges 0 – 4 and 0 – 12 plus the ‘FLAG=0’ and ‘#XMMEA_EM’ filters for the PN and MOS respectively.

Spectra were extracted from circular regions centred on the source of approximate radius $40''$ and $60''$ for the PN and MOS respectively. Backgrounds were extracted from nearby source free regions following the guidelines in Ehle et al. (2003). SAS tasks ARFGEN and RMFGEN were used to generate the appropriate response files. Background subtracted spectra were produced and grouped to a minimum of 20 counts in each bin. Spectral analysis was performed using XSPEC v11.3.0 (Arnaud 1996).

3.2 Spectral properties

Spectral fits to a simple power-law inclusive of neutral galactic absorption ($N_{\text{H}} = 1.40 \times 10^{20} \text{ cm}^{-2}$; Elvis et al. 1994) were made over the energy range 1 – 12 keV. The PN and MOS data were fitted simultaneously, but the revolution 549 and 569 observations were treated separately due to source variability. 1 – 12 keV power-law photon indices of $\Gamma = 1.88 \pm 0.05$ and $\Gamma = 1.73 \pm 0.03$ were obtained, with 2 – 10 keV fluxes of $1.22 \times 10^{-12} \text{ erg cm}^{-2} \text{ s}^{-1}$

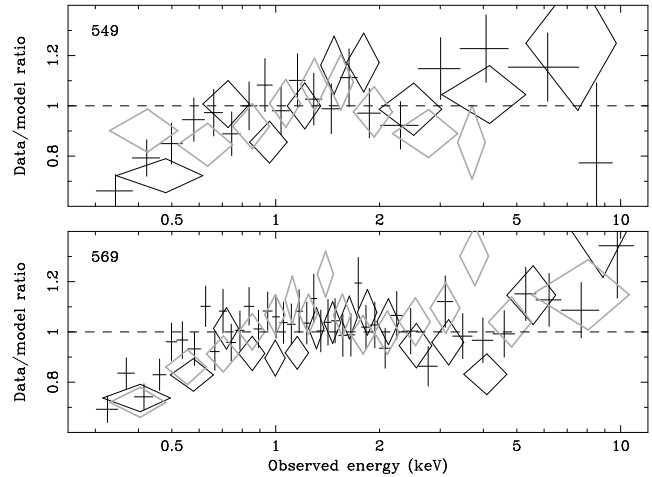


Figure 1. The upper panel shows the ratio of the revolution 549 data to a simple $\Gamma = 1.88$ power-law (including Galactic absorption of $N_{\text{H}} = 1.40 \times 10^{20} \text{ cm}^{-2}$; fitted over 1 – 12 keV). The lower panel shows the revolution 569 data to a $\Gamma = 1.73$ power-law (with the same Galactic correction and fit range). The PN data are shown in both instances as black crosses with the MOS-1/MOS-2 data as black/grey diamonds respectively.

and $1.09 \times 10^{-12} \text{ erg cm}^{-2} \text{ s}^{-1}$ respectively. Reduced chi-squared values for the fits were $\chi^2_{\nu} = 0.819$ and $\chi^2_{\nu} = 0.883$ (with $\nu = 100$ and $\nu = 283$ degrees of freedom) respectively. These can be compared to only $\chi^2_{\nu} = 1.06$ ($\nu = 385$) with an attempt to fit the same model to the data from both observations simultaneously.

A significant depression in the soft X-ray spectrum is seen when the whole 0.3 – 12 keV energy range is considered. The chi-squared statistic of the power-law models rises to $\chi^2_{\nu} = 1.245$ and $\chi^2_{\nu} = 1.302$ (for $\nu = 173$ and $\nu = 430$) respectively. Fig. 1 shows the ratio of the revolution 549 and 569 data to the 1 – 12 keV fitted power-law. Spectral flattening is clear in both observations, with a break from the power-law occurring at energies $\sim 0.6 - 1$ keV and the data/model ratio decreasing to ~ 0.7 at $\lesssim 0.4$ keV.

Even though there has been a significant decrease in flux between the observations (and possibly spectral slope variations) it remains instructive to consider the combined PN spectra in the search for spectral features which may exist at the same energy independently of other variations. To this end the PN camera good events from both observations were merged and a single spectrum extracted. Fig. 2 shows the ratio of the data to a 1 – 12 keV fitted power-law with $\Gamma = 1.77$ (plotted in the rest energy frame of the blazar). Apart from the distinctive spectral flattening there appear to be no statistically significant features.

The spectral break can be modelled in a number of ways. Table 2 shows the results of broken power-law and power-law plus absorption models. The best-fitting local absorption column density exceeds the expected galactic level at the 7-sigma level. If the excess is modelled as cold absorption at the source then column densities of $1.4 - 1.6 \times 10^{22} \text{ cm}^{-2}$ are required. Fig. 3 shows the confidence contours in the photon index and column density (for intrinsic cold absorption) for the two observations.

3.3 Variability

Background-corrected lightcurves were extracted for both observations. The good-time-interval lightcurve from the revolution 549 observation is fully consistent with a constant flux (the PN count-rate is 0.73 cts s^{-1} corresponding to $1.22 \times 10^{-12} \text{ erg cm}^{-2} \text{ s}^{-1}$).

Table 2. Summary of the spectral fits performed to the revolution 549 and 549 data. Fits were made in each case, to the PN and MOS spectra jointly over the energy range 0.3 – 12 keV. Errors indicated are 1-sigma for one interesting parameter.

Model	local N_{H} (10^{20} cm^{-2})	intrinsic N_{H} (10^{22} cm^{-2})	Γ_1	E_{break} (keV)	Γ_2	χ^2_{ν}	ν
Rev. 549 data:							
Broken power-law	1.40 (Galactic)	0	1.1 ± 0.3	0.7 ± 0.2	1.83 ± 0.03	0.851	171
power-law, free local absorption	5.0 ± 0.5	0			1.92 ± 0.05	0.840	172
power-law, free intrinsic absorption	1.40 (Galactic)	1.4 ± 0.4			1.87 ± 0.04	0.844	172
Rev. 569 data:							
Broken power-law	1.40 (Galactic)	0	0.7 ± 0.2	0.6 ± 0.1	1.71 ± 0.02	0.932	428
power-law, free local absorption	5.1 ± 0.5	0			1.79 ± 0.03	0.949	429
power-law, free intrinsic absorption	1.40 (Galactic)	1.6 ± 0.2			1.76 ± 0.02	0.931	429

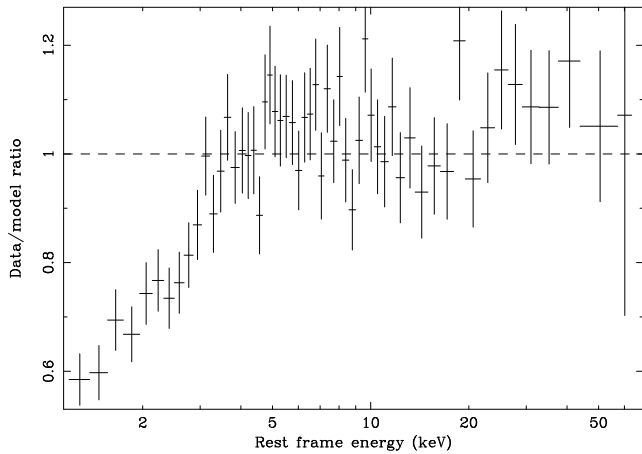


Figure 2. The combined PN camera data of both observations, plotted as a ratio to a fitted $\Gamma = 1.77$ power-law (including Galactic absorption of $N_{\text{H}} = 1.40 \times 10^{20} \text{ cm}^{-2}$). The energy has been adjusted to the source rest frame; the observed range is identical to that covered in Fig. 1.

Unfortunately the remaining ~ 60 per cent of the observation was affected by solar flare activity and reliable background subtraction could not be performed. The revolution 549 observation suffered from no flare periods and ~ 12 ks of PN data were extracted, again this is consistent (at the 90 per cent level) with a constant flux (a PN count-rate of 0.54 cts s^{-1} corresponding to $1.09 \times 10^{-12} \text{ erg cm}^{-2} \text{ s}^{-1}$). The ~ 10 per cent reduction between the observations corresponds to a variability timescale of ~ 7 days in the rest frame.

In addition to the decrease in luminosity there are differences in the spectral properties of the source between observations. The revolution 549 data are well fit (in the 1 – 12 keV range) by a simple power-law with a photon index of $\Gamma \sim 1.9$ whilst this is hardened to $\Gamma \lesssim 1.8$ during the revolution 569 observation. The break energy and soft X-ray photon index (and equivalently, the column densities in the absorption models) are in good agreement between the observations.

There would also seem to be significant variations in the spectral shape between the *XMM-Newton* and earlier observations. The continuum slopes (i.e. after correction for any soft X-ray flattening) reported by *ROSAT* and *BeppoSAX* (Boller et al. 2000; Fabian et al. 2001a) were 1.4 ± 0.2 and 1.45 ± 0.1 respectively, considerably harder than the $\sim 1.7 - 1.9$ found with *XMM-Newton*. The spectral break is characterised by the column density required of an intrinsic cold absorber, the *ROSAT* and *BeppoSAX* values of which are

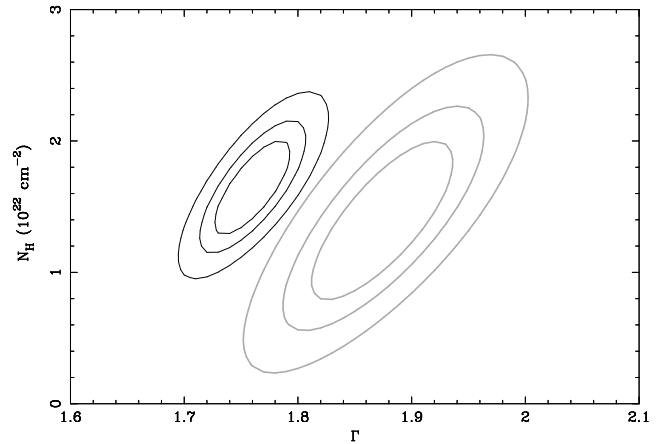


Figure 3. Confidence contours (68, 90 and 99 per cent) in the photon index and absorber column density for a power-law plus intrinsic cold absorber model (also including galactic absorption). The separate contours for revolutions 549 and 569 are shown in grey and black respectively.

$1.5 \pm 0.3 \times 10^{22} \text{ cm}^{-2}$ and $7.8^{+8.7}_{-6.0} \times 10^{22} \text{ cm}^{-2}$, consistent with each other and the $\sim 1.4 - 1.6 \times 10^{22} \text{ cm}^{-2}$ found here.

There is marginal evidence of curvature in the residuals of the *XMM-Newton* fits to the 1 – 12 keV power-law, with excesses at $\sim 1 - 2$ keV and $\sim 5 - 10$ keV and a deficit over $\sim 2 - 5$ keV (Fig. 1). The $\gtrsim 5$ keV range appears to have a harder power-law ($\Gamma \sim 1.5$), which is in better agreement with the *ROSAT* and *BeppoSAX* results. A steeper 1 – 12 keV slope and curved residuals in the *XMM-Newton* data could possibly then be the result of a $\sim 1 - 3$ keV variable excess ($\sim 5 - 20$ keV rest frame) superimposed upon the soft X-ray break.

To investigate further a difference spectrum was formed by subtracting the revolution 569 spectrum from the revolution 549 one. The difference is well-fitted by a power-law model (inclusive of Galactic absorption and intrinsic cold absorption of $N_{\text{H}} = 1.5 \times 10^{22} \text{ cm}^{-2}$) with a spectral slope of $\Gamma = 2.3 \pm 0.3$. A two power-law model (again inclusive of Galactic and intrinsic absorption) is also an acceptable fit to both data sets. The soft power-law component has $\Gamma \sim 1.8 - 2.6$ and the hard power-law has $\Gamma \lesssim 1.7$.

The curved residuals, 1 – 3 keV excess and the success of the two power-law model point to the intriguing possibility that the spectrum may contain an additional component. The steepness ($\Gamma \sim 2.3$) of the soft component is consistent with the high-energy cut-off of a second inverse-Compton contribution. Possibilities for such a component are an underlying pile-up in the EC seed photon

distribution (see 4.2), an EC component with a different external photon source, SSC emission or a bulk Compton component due to inverse-Compton scattering from a cold electron population.

4 DISCUSSION

There are two main possibilities for the origin of the spectral flattening observed in GB B1428+4217. The first, and our favoured explanation, is that the flattening is due to excess intrinsic absorption. The second hypothesis attributes the effect to a break in the underlying blazar emission continuum. These two alternatives are now discussed separately.

4.1 Absorption

A galactic origin to the excess column density is extremely unlikely; it would require a factor ~ 3.6 increase in the galactic column density, highly localised in the direction of GB B1428+4217. Intergalactic absorption is also highly unlikely, the only possibility being a line of sight that passes through two or more very high column density damped Ly- α systems for which the probability is very low (O’Flaherty & Jakobsen 1997; Zwaan et al. 1999). If an absorber is the origin of the X-ray flattening it must therefore be metal-rich and intrinsic to the source. A cold absorber model requires a column density in the region $1.4 - 1.6 \times 10^{22} \text{ cm}^{-2}$.

A warm (ionized) absorber is able to reproduce both low UV and high X-ray column densities. Photoionized gas could produce significant photoelectric absorption in the soft X-ray band (mainly due to oxygen and neon species) whilst remaining transparent at UV wavelengths (hydrogen/helium both ionized). Additionally, any dust grains could be destroyed by the intense photon-flux, resulting in low levels of extinction in the UV band.

The photoionization code CLOUDY (Ferland et al. 1998) was used to model the warm absorber hypothesis. Fig. 4 shows the confidence contours in the warm absorber ionization parameter and column density for the two separate observations. Neither set of contours strongly constrains the ionization parameter provided that $\xi \lesssim 10^2 \text{ erg cm s}^{-1}$. The column density is in the range $10^{22} \lesssim N_{\text{H}} \lesssim 10^{23} \text{ cm}^{-2}$.

It is difficult to break this degeneracy with X-ray observations: The conclusive signature of a warm absorber would be the detection of photoelectric absorption edges, principally those arising from O/Ne. Due to the high- z of the source however, these features are redshifted out of the observed band to energies $\lesssim 0.2 \text{ keV}$. A strong discriminator would be evidence of Lyman-limit absorption at 5217 \AA (the present optical data start at 5970 \AA). This would place constraints on the neutral hydrogen column density and thus on the ionization state of the absorber. The lack of an optically-thick Lyman-limit system would immediately place an upper limit to the H I column density of $\sim 10^{17} \text{ cm}^{-2}$, requiring the warm absorption model to have an ionization parameter $\xi \gtrsim 1 \text{ erg cm s}^{-1}$.

4.2 Intrinsic spectral properties

The revolution 549 and 569 spectra can be acceptably fitted with a broken power-law model with a break at an energy $\sim 0.6 - 0.7 \text{ keV}$ down to a flat spectral index $\sim 0.7 - 1.1$. In the rest frame (Fig. 2) the break energy is $\sim 4 \text{ keV}$ and is very distinct, occurring over a range of $\sim 2 \text{ keV}$. The $z = 4.4$ blazar PMN J0525–3343 is similar with a sharp spectral break at a rest frame energy of $\sim 4.5 \text{ keV}$ over an energy range $\lesssim 5 \text{ keV}$.

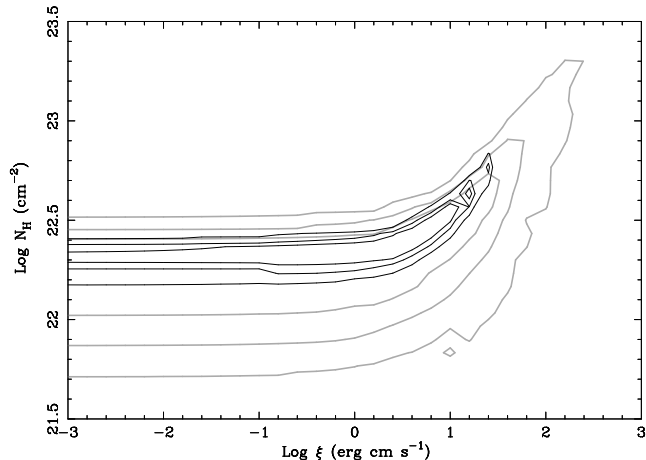


Figure 4. Confidence contours (68, 90 and 99 per cent) in the photon index and column density for a power-law plus intrinsic cold absorber model (also including galactic absorption). The separate contours for the revolution 549 and 569 observations are shown in grey and black respectively.

The dominant emission components in blazars are beamed synchrotron radiation from the jet (peaking in the infra-red to soft X-ray band) and a high-energy component (dominating the hard X-ray to γ -ray regimes). The high-energy emission arises through the inverse Comptonization of soft photons by highly relativistic electrons in the jet plasma. Sources of the soft photons are the nuclear optical/UV emission or the local synchrotron radiation within the jet. For the brightest blazars (such as GB B1428+4217 and PMN J0525–3343) the first, known as the ‘external Compton’ (EC) mechanism, is dominant (Sikora et al. 1994).

A flattening in the spectrum could be expected if there was a low energy cut-off in the energy distribution of the electron population in the jet. In the case of the EC process it is also possible to produce a spectral break by requiring the seed photon distribution to be sharply peaked at and/or rapidly decline below a certain frequency. There are several problems with these explanations: Firstly, there is no evidence of any spectral breaks in the spectra of nearby radio-loud quasars, and secondly, there seems to be no plausible way to account for the sharpness of the break (only a few keV in the rest frame). For a more detailed discussion of the break-producing mechanisms see e.g. Fabian et al. (2001b).

4.3 Comparisons with other objects

Fig. 5 shows the rest frame combined PN spectrum of GB B1428+4217 (as a ratio to the power-law above the spectral break) along with the equivalent result for PMN J0525–3343 (Worsley et al. 2004). The agreement in the position and structure of the break is remarkable. Since the plots are of ratios to the model the instrumental response (and Galactic absorption) have been removed. In both cases the break from the power-law occurs over a range of $\lesssim 5 \text{ keV}$ in the source frame and to a photon index of $\Gamma \sim 1$. Both also show a steeper drop in the flux at 3 keV .

If the spectral flattening is indeed due to warm absorption then the absorbers for GB B1428+4217 and PMN J0525–3343 are almost identical in column density (of $\sim 2 - 4 \times 10^{22} \text{ cm}^{-2}$). There is also evidence for a similar column in the *XMM-Newton* observations of RX J1028.6–0844 (Grupe et al. 2004) where joint fits to the *XMM-Newton* and previous *ASCA* data (Yuan et al. 2000) are consistent with an excess intrinsic column density of $\sim 1 \times 10^{22} \text{ cm}^{-2}$.

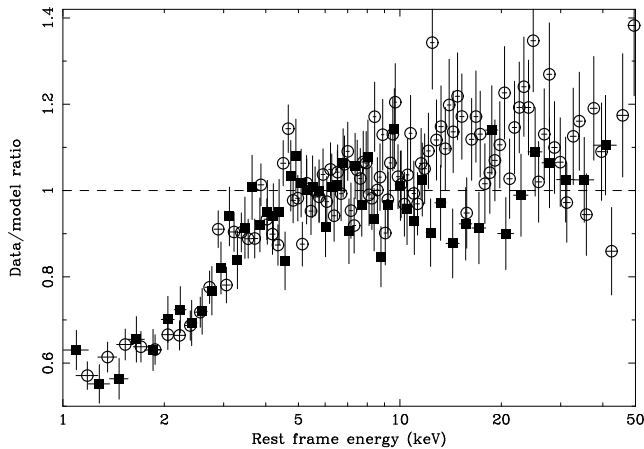


Figure 5. The ratio of combined PN camera spectra to a hard-band fitted power-law. The filled squares show the data for GB B1428+4217; the power-law has $\Gamma = 1.77$ and was fitted over the observed 1 – 12 keV range. The open circles show the data for PMN J0525–3343; the power-law has $\Gamma = 1.71$ and was fitted over the observed 2 – 12 keV range. The spectra are plotted in their respective rest frame energies. The spectra have also been renormalised to a data/model ratio of unity over the 5 – 10 keV rest frame range.

5 CONCLUSIONS

We have studied the X-ray spectrum of the high-redshift, radio-loud blazar GB B1428+4217, providing definitive confirmation of the soft X-ray spectral flattening as previously observed with *ROSAT* and *BeppoSAX*. The flattening is not consistent with Galactic or intergalactic absorption and we propose that the effect is due to an absorber that is intrinsic to the source, or to an underlying break in the blazar continuum.

A continuum break is highly speculative given the present lack of knowledge concerning emission processes in the nuclear regions. Continuum breaks are not seen in nearby radio-loud objects where they should be readily detectable and there is no satisfactory way to account for the sharpness of the break seen. An intrinsic absorber is therefore our favoured explanation. Cold absorption requires a column density $N_{\text{H}} \sim 1.4 - 1.6 \times 10^{22} \text{ cm}^{-2}$, whilst a warm absorber could have a column density of up to $\sim 10^{23} \text{ cm}^{-2}$ and an ionization parameter $\xi \sim 10^2$. X-ray data alone are unable to distinguish between a warm or cold absorber model. Good constraints are expected from future optical observations which could place strong limits on the neutral hydrogen column density.

It is interesting to note the parallels with the blazar PMN J0525–3343 (Worsley et al. 2004) i.e. a relatively blue UV continuum with strong Ly- α and C IV emission lines as well as the flat hard X-ray spectral slope and the remarkably similar form of the soft X-ray depression. The PMN J0525–3343 X-ray data are consistent with both warm/cold absorption but optical observations rule out a cold absorber scenario. The lack of significant reddening in the UV spectra of both objects is consistent with a dust-free warm absorber.

Comparisons can also be drawn to the $z = 3.27$ radio-loud quasar PKS 2126–0158 which also shows definite soft X-ray absorption (Ferrero & Brinkmann 2003; Fiore et al. 2003). Both warm and cold absorbers are consistent although ionized absorption is again most able to explain the lack of significant UV reddening. The implied iron abundance of a warm absorber however is at odds with the super-solar abundances implied by broad emission lines.

The spectrum of GB B1428+4217 are suggestive of an additional component contributing to an excess of emission in the $\sim 5 - 10$ keV rest-frame energy range. There are a number of possibilities for the emission including a pile-up in the electron energy distribution or a feature caused by bulk Comptonization, however the detection is marginal and further work is required.

6 ACKNOWLEDGMENTS

Based on observations with *XMM-Newton*, an ESA science mission with instruments and contributions directly funded by ESA Member States and the USA (NASA). MAW acknowledges support from PPARC. ACF thanks the Royal Society for support. AC thanks the Italian MIUR and INAF for financial support.

REFERENCES

- Arnaud K. A., 1996, in ASP Conf. Ser. 101: Astronomical Data Analysis Software and Systems V, p. 17
- Boller T., Fabian A. C., Brandt W. N., Freyberg M. J., 2000, MNRAS, 315, L23
- Cappi M., Matsuoka M., Comastri A., Brinkmann W., Elvis M., Palumbo G. G. C., Vignali C., 1997, ApJ, 478, 492
- Crenshaw D. M., Kraemer S. B., Bogges A., Maran S. P., Mushotzky R. F., Wu C., 1999, ApJ, 516, 750
- Ehle M. et al., 2003, The XMM-Newton Users' Handbook 2.1
- Elvis M., Lockman F. J., Fasnacht C., 1994, ApJS, 95, 413
- Fabian A. C., Brandt W. N., McMahon R. G., Hook I. M., 1997, MNRAS, 291, L5
- Fabian A. C., Celotti A., Iwasawa K., Ghisellini G., 2001a, MNRAS, 324, 628
- Fabian A. C., Celotti A., Iwasawa K., McMahon R. G., Carilli C. L., Brandt W. N., Ghisellini G., Hook I. M., 2001b, MNRAS, 323, 373
- Fabian A. C., Celotti A., Pooley G., Iwasawa K., Brandt W. N., McMahon R. G., Hoenig M. D., 1999, MNRAS, 308, L6
- Fabian A. C., Iwasawa K., McMahon R. G., Celotti A., Brandt W. N., Hook M., 1998, MNRAS, 295, L25
- Ferland G. J., Korista K. T., Verner D. A., Ferguson J. W., Kingdon J. B., Verner E. M., 1998, PASP, 110, 761
- Ferrero E., Brinkmann W., 2003, A&A, 402, 465
- Fiore F., Elvis M., Giommi P., Padovani P., 1998, ApJ, 492, 79
- Fiore F., Elvis M., Maiolino R., Nicastro F., Siemiginowska A., Stratta G., D'Elia V., 2003, A&A, 409, 57
- Grupe D., Mathur S., Wilkes B., Elvis M., 2004, AJ, 127, 1
- Hook I. M., McMahon R. G., 1998, MNRAS, 294, L7
- O'Flaherty K. S., Jakobsen P., 1997, ApJ, 479, 673
- Péroux C., Storrie-Lombardi L. J., McMahon R. G., Irwin M., Hook I. M., 2001, AJ, 121, 1799
- Reeves J. N., Turner M. J. L., 2000, MNRAS, 316, 234
- Reynolds C. S., 1997, MNRAS, 286, 513
- Sikora M., Begelman M. C., Rees M. J., 1994, ApJ, 421, 153
- Worsley M. A., Fabian A. C., Turner A., Celotti A., Iwasawa K., 2004, MNRAS, in press (astro-ph/0310366)
- Yuan W., Matsuoka M., Wang T., Ueno S., Kubo H., Mihara T., 2000, ApJ, 545, 625
- Zwaan M. A., Verheijen M. A. W., Briggs F. H., 1999, Publications of the Astronomical Society of Australia, 16, 100